ConTopo: Non-Rigid 3D Object Retrieval using Topological Information guided by Conformal Factors

K. Sfikas[†1], I. Pratikakis[2] and T. Theoharis[1]

[1]Department of Informatics & Telecommunications, University of Athens, Greece
[2]Department of Electrical & Computer Engineering, Democritus University of Thrace, GR-67100, Xanthi, Greece

Abstract

Combining the properties of conformal geometry and graph-based topological information for 3D object retrieval, a non-rigid 3D object descriptor is proposed, which is both robust and efficient in terms of retrieval accuracy and computation speed. In previous works, graph-based methods for non-rigid 3D object retrieval, have shown high discriminative power and robustness, while geometry-based methods, have proven to be tolerant to noise and pose. In this work, we present a 3D object descriptor that combines the above advantages.

Categories and Subject Descriptors (according to ACM CCS): I.3.5 [Computer Graphics]: Computational Geometry and Object Modeling—i.3.7 [Computer Graphics]: Three-Dimensional Graphics and Realism—

1. Introduction

The increasing availability of 3D objects makes content based retrieval a key operation. Retrieval methods are based on the creation of a shape descriptor that faithfully encodes the shape of the objects in an efficient manner. 3D object descriptors can be classified into two main categories: rigid and non-rigid. Over the last years, a lot of research effort has successfully addressed rigid 3D shape descriptors exploiting inter-class variability. However, in the case of intra-class variability non-rigid 3D object descriptors are more effective where the objects of the class can assume a variety of transformations, including deformations.

In this paper we present a non-rigid 3D object descriptor by combining two concepts: (i) the geometry-based discrete conformal factor by Ben-Chen and Gotsman [BCG08], which provides geometry information and is tolerant to pose and noise, and (ii) graphs [HSKK01, BGSF08], which provide topology information and have shown high discriminative power and robustness.

The remainder of the paper is structured as follows. In section 2, related work in 3D shape descriptors, categorized into rigid and non-rigid, is discussed. In section 3, the proposed method is given, including a detailed description of the combined approach along with a brief introduction for each constituent methodology, namely conformal mappings and graphs. Combining those theories, the proposed 3D shape descriptor is presented. Section 4 presents the evaluation methodology along with the experimental results and the related discussion. Finally conclusions are drawn in section 5.

2. Related Work

Research in the field of 3D shape descriptors has advanced significantly over the past few years, leading to a number of different categorizations [SMKF04, TV08, BP06] according to the features and/or representations used. One such categorization is into rigid and non-rigid 3D object descriptors.

2.1. Rigid 3D Object Descriptors

Rigid 3D object descriptors usually address inter-class 3D object retrieval.

One of the most cited methods for 3D object retrieval, based on the extraction of features from 2D representations of the 3D objects, was the LightField descriptor, proposed by Chen et al. [CSTO03]. This descriptor comprises of Zernike moments and Fourier coefficients computed on a set of projections taken from the vertices of a dodecahedron. The SH-GEDT descriptor proposed by Kazhdan et

† This work has been funded by scholarship from the Greek State Scholarship Foundation (I.K.Y.)

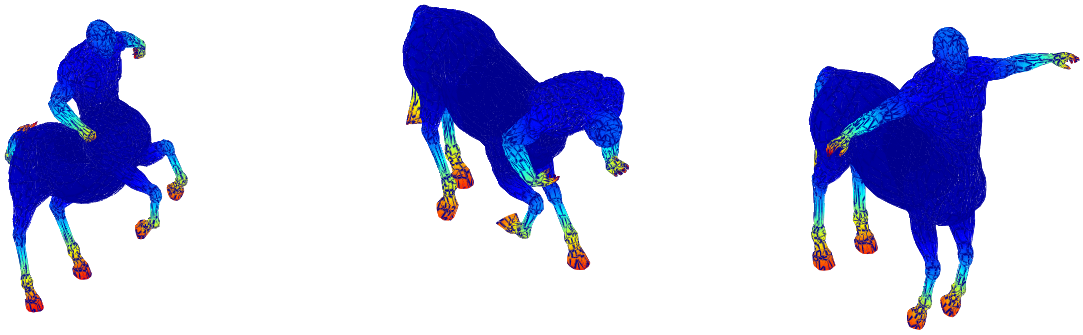

Figure 1: Three sample models from the class 'Centaur' of the TOSCA dataset, color-coded with the corresponding conformal factors.

al. [KFR03] is a volumetric representation of the Gaussian Euclidean Distance Transform of a 3D object, expressed by norms of spherical harmonic frequencies. Papadakis et al. [PPPT08] proposed a hybrid descriptor formed by combining features extracted from a depth-buffer and spherical-function based representation, with enhanced translation and rotation invariance properties. Sfikas et al. enhanced this method by the addition of a symmetry based new pose normalization method [STP10]. Papadakis et al. in [PPTP09] proposed PANORAMA, a 3D shape descriptor that uses a set of panoramic views of a 3D object which describe the position and orientation of the object's surface in 3D space. For each view the corresponding 2D discrete Fourier Transform and the 2D discrete Wavelet Transform are computed.

2.2. Non-Rigid 3D Object Descriptors

Non-rigid 3D object descriptors can effectively deal with intra-class 3D object retrieval, where the objects of the class can assume a variety of transformations, including deformations.

A large number of methods are based on the discrete Laplace-Beltrami operator. Reuter at al. [RWP06] compare two triangulated surfaces by computing the distance between two isometry-invariant feature vectors given by the first n eigenvalues of the Laplace-Beltrami operator. Similarly, Rustamov [Rus07] uses the eigenvectors of the Laplace-Beltrami operator. Zaharia and Preteux [ZP02] presented the 3D shape spectrum descriptor which is the histogram that describes the angular representation of the first and second principal curvature along the surface of the 3D object. Xiang et al. [XHGC07] use the histogram of the solution to the volumetric Poisson equation $\nabla 2U = -1$ (which involves the Laplace-Beltrami operator) as a pose invariant shape descriptor. In a similar manner, Ben-Chen and Gotsman [BCG08], working on the boundary surface of the 3D shape, create a descriptor that maps the local curvature characteristics of the 3D object. The histogram of the solution to the conformal factor equation $\nabla 2\phi$ is used. The same principles were also used by Wang et al. [WWJ*06] for face recognition using 3D conformal maps.

Some non-rigid shape descriptors are derived from geodesic distances on the mesh, which are invariant to isometric transformations. Elad and Kimmel [EK03] proposed a canonical representation for triangulated surfaces: a surface in R^3 is transformed into canonical coordinates in the Euclidean space R^m by applying multi-dimensional scaling. In this canonical representation the geodesic distances on the original surface are approximated by the corresponding Euclidean distances. The matching problem of non-rigid and deformed objects is then reduced to the problem of matching rigid objects embedded in R^m, which can be approached with well-known algorithms. Jain and Zhang [JZ07] compare non-rigid objects by matching spectral embeddings that are derived from the eigenvectors of affinity matrices, computed by considering geodesic distances. A non-rigid descriptor based on histograms of surface functions is presented by Gal et al. [GSCO07], where two scalar functions are used on the mesh. Carlsson et al. [CZCG04] compared barcode descriptors of point clouds computed by using the persistence homology theory. Dey et al. [DGG03] compared noisy point clouds, by matching signatures extracted from segmented parts of the point sets by making use of Morse theory. In [MDTS09], Mademlis et al. proposed a novel shape descriptor based on the impact that the 3D objects have when they are exposed to a specific type of force field (i.e. the Newtonian or the Coulombian fields). The 3D objects are initially voxelized and subsequently the histograms of the field factors are compared.

Zhang et al. [ZSM*05] consider the use of medial surfaces to compute an equivalent directed acyclic graph of an object. In the work of Sundar et al. [SSGD03], the 3D object passes through a thinning process producing a set of skeletal points, which form a directed acyclic graph by applying the minimum spanning tree algorithm. The P3DS descrip-

tor developed by Kim et al. [KPYL05] uses an attributed relational graph whose nodes correspond to parts of the object that are represented using ellipsoids and the similarity is computed by employing the earth mover's distance. Hilaga et al. [HSKK01] presented a technique to match the topology of triangulated models, by comparing Multiresolution Reeb Graphs (MRGs). Their algorithm for matching two MRGs is a coarse-to-fine strategy, which searches the node pairs providing the largest value of similarity while maintaining topological consistency. Similarly to [HSKK01], Hamza and Krim [HK03] considered a discrete approximation of the global squared geodesic distance function. The dissimilarity between two objects was calculated by computing the Jensen-Shannon divergence between the corresponding statistical shape descriptors. Tung and Schmitt [TS05] used geodesic distances for building an MRG and merge the graph geometrical and visual information to calculation of shape similarity between models. In recent research works, Tierny et al. [TVD09] compare 3D models by extracting partial signatures from disk or annulus-like charts using Reeb graph topology. Bronstein et al. [BBK*10] instead of using geodesic distances for extracting shape signatures, they exploit the properties of diffusion distances within the Gromov-Hausdorff framework. Biasotti et al. [BPS*10] described a method for the characterization of shapes by using a set of patches, which are automatically tiled and stitched, in order to approximate the original shape. Reeb graphs are used for the definition of the main shape features that drive the approximation process.

3. The Proposed Method

In the sequel, a non-rigid 3D object descriptor, using graph topological structure driven by the discrete conformal factors, introduced by Ben-Chen and Gotsman [BCG08] will be presented. We shall briefly introduce both of the aforementioned concepts and then describe the proposed combined scheme.

Before we proceed, let us define a triangular mesh $M = \{V, F, E\}$, represented by the set of vertices V, the set of faces F and the set of edges E connecting neighboring vertices. Optionally, the set of the boundary vertices B could be defined. For a vertex v_i, $V_1(i)$ denotes the 1-ring set of adjacent vertices to v_i and $F_1(i)$ denotes the 1-ring set of adjacent faces to v_i.

3.1. The Discrete Conformal Factor

Ben-Chen and Gotsman in [BCG08] have introduced the discrete conformal factor for a 3D mesh, which is used as a non-rigid shape descriptor. The conformal factor ϕ_i at a vertex v_i of the triangular 3D mesh M is the solution to the following discrete linear equation (see Figure 1):

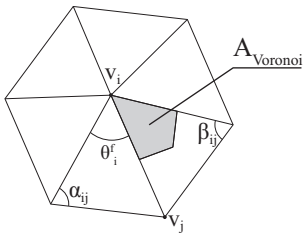

Figure 2: Adjacent faces of vertex v_i at 1-ring neighborhood. Angle θ_i^f and $A_{Voronoi}$ region are also presented.

$$\phi_i = \frac{k_i^{targ} - k_i^{orig}}{\mathcal{L}(v_i)} \tag{1}$$

where $\mathcal{L}(v_i)$ denotes the discrete Laplace - Beltrami function, at vertex v_i, with cotangent weights, defined in [MDSB02]:

$$\mathcal{L}(v_i) = \frac{1}{2A_{Mixed}} \sum_{j \in V_1(i)} (\cot\alpha_{ij} + \cot\beta_{ij})|v_i - v_j| \tag{2}$$

where A_{Mixed} denotes as the mesh surface area around a vertex v_i, which is computed as shown in Algorithm 1 (see also Figure 2).

Algorithm 1 Pseudo-code for the calculation of the surface area of region A_{Mixed} of vertex v_i on an arbitrary mesh

```
A_Mixed = 0
for f ∈ F_1(i) do
    if f is non-obtuse then
        A_Mixed += A_Voronoi
    else
        if the angle of f at v_i is obtuse then
            A_Mixed += area(f)/2
        else
            A_Mixed += area(f)/4
        end if
    end if
end for
return A_Mixed
```

$area(f)$ denotes the triangular area of face f based on a standard estimation method (Heron's formula). $A_{Voronoi}$ denotes the surface area contribution of a single non-obtuse triangle in $F_1(i)$ (see Figure 2).

$$A_{Voronoi} = \frac{1}{8} \sum_{j \in F_1(i)} (\cot\alpha_{ij} + \cot\beta_{ij})\|v_i - v_j\|^2 \tag{3}$$

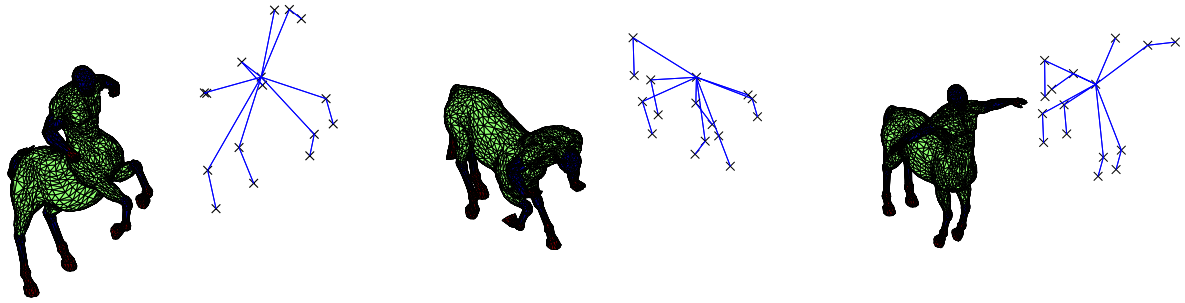

Figure 3: Examples of partitionings and the corresponding graphs of 3D meshes from the class 'Centaur' of the TOSCA dataset using the discrete conformal factor as μ function.

where α_{ij} and β_{ij} denote the two angles opposite to the common edge $\widehat{v_i v_j}$ (see Figure 2).

In (1), k_i^{orig} is defined as the discrete Gaussian Curvature at vertex v_i of the triangular 3D mesh:

$$k_i^{orig} = \begin{cases} 2\pi - \sum\limits_{f \in F_1(i)} \theta_i^f, & v_i \in V \backslash B \\ \pi - \sum\limits_{f \in F_1(i)} \theta_i^f, & v_i \in B \end{cases} \quad (4)$$

The first case of equation (4) is used for vertices of the triangular mesh whose 1-ring of adjacent faces is closed, whereas the second case is used for vertices that belong to the boundary of the triangular mesh (if such boundary exists). θ_i^f is the angle near vertex v_i of face f (see Figure 2).

In (1), k_i^{targ} denotes the uniform Gaussian Curvature:

$$k_i^{targ} = \left(\sum_{j \in V} k_j^{orig} \right) \frac{\sum\limits_{f \in F_1(i)} \frac{1}{3} area(f)}{\sum\limits_{f \in F} area(f)} \quad (5)$$

k_i^{targ} assigns to each vertex a portion of the total curvature of the mesh.

3.2. Graph Construction

A graph can be used as a topological map that represents the skeletal structure of an object with arbitrary dimensions. Reeb graphs are an example of methods for the characterization of 3D mesh topological information [HSKK01, CMEH*04, BGSF08]. Here, in similar manner, we will define a graph, that captivates the topological structure of an arbitrary 3D mesh:

The nodes of the graph represent connected components, while the edges of the graph describe the connectivity between adjacent connected component sets. Each connected component is composed of 3D mesh faces that belong to the same level-set (i.e. have the same label) and are also pathwise-connected (i.e. there exists a continuous path that connects each face of the connected component to every other face that belongs to the same connected component). The level-sets are defined by the μ function, which labels the faces of the 3D mesh, based on a selection of characteristics (see also Figure 4).

It is evident that the selection of μ function is critical for the construction of the corresponding graph. Among the various types of μ and related graphs, one of the simplest examples is a height function [dBvK93, SKK91, TSK97, TV98]. Other options include functions that measure the distance between each vertex on the surface of a 3D mesh and an approximation of its center of mass and/or using other geodesic properties of the 3D mesh.

Driven by the work of Ben-Chen and Gotsman and properties of graphs, discrete conformal factors appear to be a good candidate for the μ function to guide the graph construction (Figure 3). This is mainly due to the stability and robustness of the discrete conformal factors when used as a non-rigid 3D shape signature [BCG08].

At this point, note that the computation of the graph is based on the triangle set F of the 3D mesh and not on the corresponding vertex set. Therefore, it is necessary to map the magnitude of the discrete conformal factors from the vertices to the faces of the triangulated mesh. To achieve this, for each triangular face we aggregate the conformal factor values of the three vertices ϕ_i^f:

$$\phi^f = \sum_{i=1}^{3} \phi_i^f, \quad f \in F \quad (6)$$

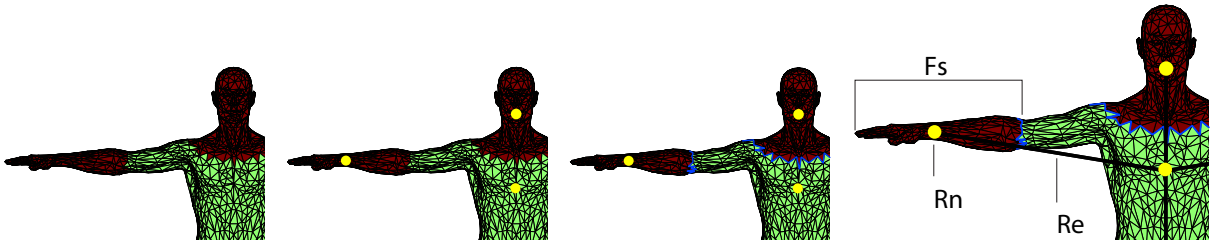

Figure 4: Detailed steps for the construction of the graph for a 3D mesh. Sample **Rn**, **Re**, and **Fs** are illustrated.

The algorithm for the computation of the graph is composed of the following steps:

- Quantization of the 3D mesh surface, based on the values of the μ function computed over the 3D mesh's faces, into q discrete partitions (Figure 4a).
- Definition of connected component sets and their representative points (centers of mass) at each mesh partition (Figure 4b).
- Estimation of boundary edges between adjacent connected components (Figure 4c).
- Connection between neighboring nodes that represent adjacent connected components by graph edges (Figure 4d).

In our implementation we have selected $q = 3$, which creates a three-level graph. This choice has been experimentally determined as it yields good results while simultaneously preserving acceptable computational speed. During the graph construction procedure, if any *small* connected component sets occur, then these sets are removed as outliers, in order to ensure the coherence of the corresponding graphs. In our implementation we define a *small* connected component set if it is composed of less than 2% of the 3D mesh surface. The outcome of the graph construction is a set of matrices that represent its structure:

Rn: The nodes of the graph.
Re: The edges connecting the **Rn** of the graph. **Re** are represented by an $N \times N$ adjacency matrix, where N equals to the number of **Rn**.
Fμ: The mean value of μ function at each connected component.
Fs: The set of faces (triangles) in each connected component. Each **Fs** is represented by a corresponding **Rn**.
Fs$_{area}$**:** The area of the faces that belong to each **Fs**. **Fs**$_{\mathbf{area}}$ is normalized with respect to the total area of the 3D mesh.

3.3. Mesh Matching

Triangular mesh matching has two prongs: geometry-based and topology-based.

The topological matching procedure compares the graphs of two meshes. This procedure checks whether the two graphs are topologically equivalent. To achieve this, we apply the graph matching technique presented in [SSA08] over the graphs of triangular meshes M_1, $G_1 = (Rn_1, Re_1, F\mu_1)$ and M_2, $G_2 = (Rn_2, Re_2, F\mu_2)$, respectively. The goodness-of-fit criterion is the number of unmatched graph nodes, normalized by the total number of nodes of G_1 and G_2 and leads to the calculation of $sim_{topo}(M_1, M_2)$.

In addition to the topological matching procedure, geometry-based matching further enhances the discriminative power of the algorithm. To achieve geometry-based matching each **Fs**$_{\mathbf{area}}$ is compared to all **Fs**$_{\mathbf{area}}$ values of the second triangular mesh and vice versa. The average value of the best matching scores is kept:

$$\begin{aligned} &sim_{geo}(M_1, M_2) = \\ &\frac{1}{2}\Big(\frac{1}{N_1}\sum_{k=1}^{N_1} \min_{i=1..N_1, j=1..N_2} (|Fs_{area}(i) - Fs_{area}(j)|) + \\ &\frac{1}{N_2}\sum_{l=1}^{N_2} \min_{j=1..N_2, i=1..N_1} (|Fs_{area}(j) - Fs_{area}(i)|)\Big) \end{aligned} \tag{7}$$

where N_1, N_2 the number of **Fs** in triangular meshes M_1, M_2 respectively.

Combining sim_{topo} and sim_{geo} gives us the final measure for 3D mesh matching:

$$match(M_1, M_2) = 0.5 \cdot sim_{topo}(M_1, M_2) + 0.5 \cdot sim_{geo}(M_1, M_2) \tag{8}$$

As shown in Eq. (8), both measures are equally weighted for the calculation of the final match. The range of $match(M_1, M_2)$ lies in $[0, 1]$, where 0 represents 100% similarity.

4. Evaluation

In this section we show the performance results of the proposed non-rigid 3D shape descriptor (ConTopo) on the following datasets: (i)TOSCA dataset [BBK06, BBK08]

(parts of which are also used in the SHREC'10 *Correspondence* and *Feature Detection and Description* tracks), (ii) SHREC'07 watertight models dataset [GBP07].

On the first dataset we compared against the non-rigid discrete Conformal Factor (CF) descriptor [BCG08] and the rigid LightField (LF) [CSTO03] and Spherical Harmonics (SH) [KFR03] descriptors. On the second dataset we compared against the non-rigid discrete Conformal Factor (CF) descriptor, and the augmented Multiresolution Reeb Graph (aMRG) method [TS05] (see also related work in Section 2). The LF and SH benchmark code is publicly available, the CF code was obtained from the author of [BCG08], whom we gratefully acknowledge, while the aMRG code is not publicly available and therefore, the original graphs from the SHREC'07 competition were used instead, since it was necessary for making a comparison [GBP07] and [BCG08].

Our experimental evaluation is based on Precision-Recall plots for the classes of the corresponding datasets. For every query object that belongs to a class C, recall denotes the percentage of objects of class C that are retrieved and precision denotes the proportion of retrieved objects that belong to class C over the total number of retrieved objects. The best score is 100% for both quantities.

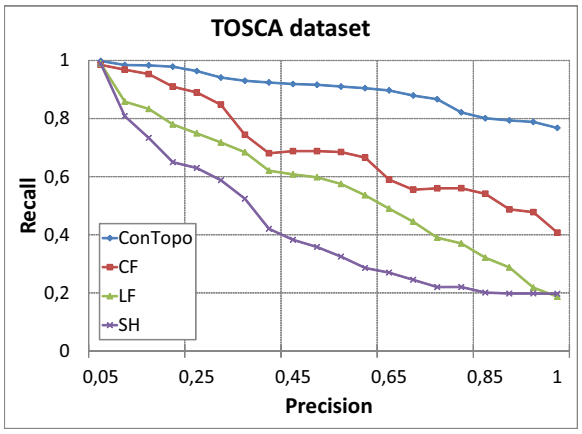

Figure 5: The average P-R scores for the TOSCA dataset. Illustrated methods are the proposed non-rigid descriptor (ConTopo), the discrete Conformal Factor descriptor (CF) and the rigid LightField (LF) and Spherical Harmonics (SH) descriptors.

In Figure 5, in accordance to the experimental results shown in [BCG08], we illustrate the P-R plots for the complete TOSCA dataset for the proposed (ConTopo) non-rigid descriptor, the discrete Conformal Factor descriptor and two state-of-the-art rigid descriptors: the LightField (LF) and the Spherical Harmonics (SH) descriptor. The P-R scores of the methods clearly illustrate the increased accuracy of ConTopo. Furthermore, Figure 7 shows the corresponding P-R scores for the same methods of representative classes of the TOSCA dataset.

According to the SHREC'07 classification scheme, the dataset, composed of 400 3D objects, is classified into 20 classes, each of which contains 20 objects. Figure 6 illustrates the P-R plot for the complete dataset and Figure 8 shows the P-R plots for some of its classes. These plots illustrate that the proposed method performs better than the discrete Conformal Factor approach while its performance against aMRG is mixed.

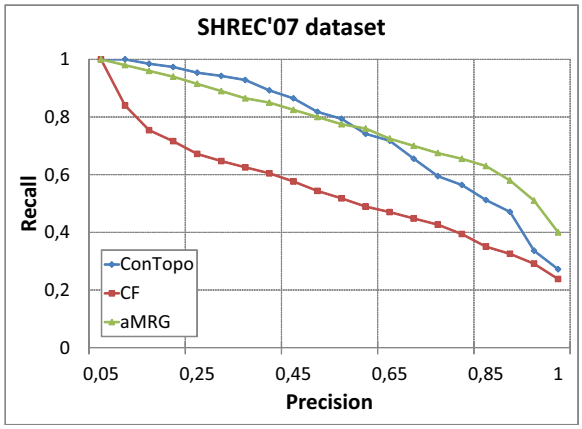

Figure 6: The average P-R scores for the SHREC'07 dataset. Illustrated methods are the proposed non-rigid descriptor (ConTopo), the discrete Conformal Factor (CF) and the aMRG method.

The proposed method was tested on a Core2Quad 2.5 GHz system, with 6 GB of RAM, running Matlab R2010b. The average computational time for a 10,000 vertex 3D mesh is about 0.6 seconds. The search in SHREC'07 dataset, is completed in about 210 seconds.

5. Conclusions

We have presented a new approach on non-rigid 3D shape descriptors by utilizing the properties of both the discrete conformal factor and graphs. The proposed method shows improved performance over the discrete Conformal Factor, as well as state-of-the-art rigid descriptors, like LightField and Spherical Harmonics on the TOSCA dataset. Its results are competitive against the Multiresolution Reeb Graph approach on the SHREC'07 dataset.

References

[BBK06] BRONSTEIN A. M., BRONSTEIN M. M., KIMMEL R.: Efficient computation of isometry-invariant distances between surfaces. *SIAM J. Sci. Comput. 28* (September 2006), 1812–1836. 5

[BBK08] BRONSTEIN A., BRONSTEIN M., KIMMEL R.: *Numerical Geometry of Non-Rigid Shapes*, 1 ed. Springer Publishing Company, Incorporated, 2008. 5

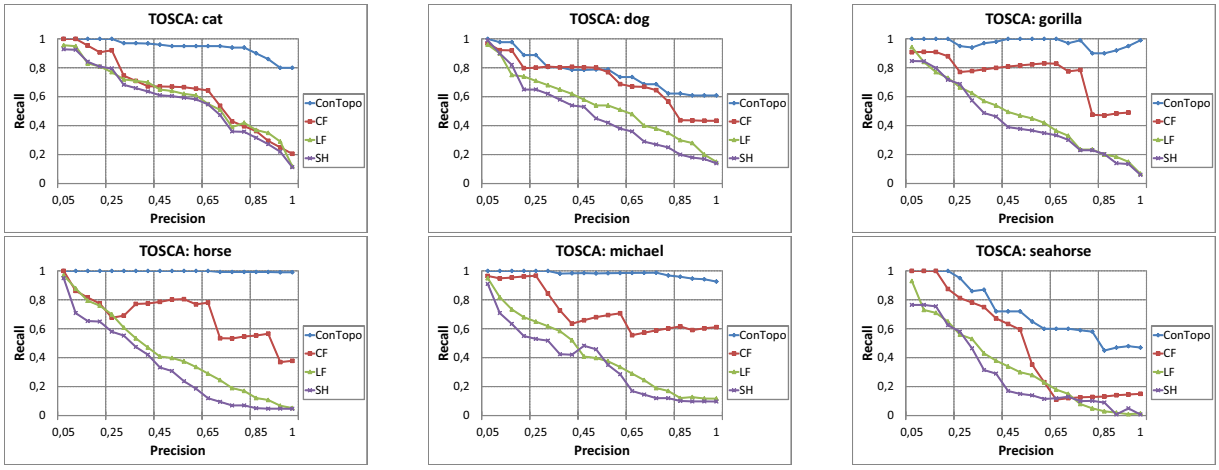

Figure 7: The P-R scores for six sample classes of the TOSCA dataset. Illustrated methods are the proposed non-rigid descriptor (ConTopo), the discrete Conformal Factor (CF), the LightField (LF) and the Spherical Harmonics (SH) descriptors.

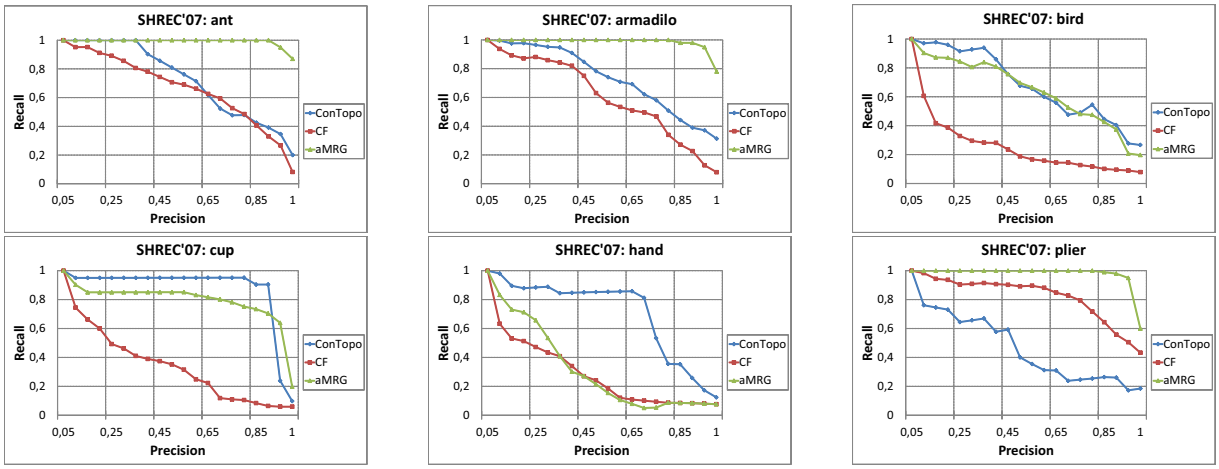

Figure 8: The P-R scores for six sample classes of the SHREC'07 dataset. Illustrated methods are the proposed non-rigid descriptor (ConTopo), the discrete Conformal Factor (CF) and the aMRG method.

[BBK*10] BRONSTEIN A. M., BRONSTEIN M. M., KIMMEL R., MAHMOUDI M., SAPIRO G.: A gromov-hausdorff framework with diffusion geometry for topologically-robust non-rigid shape matching. *Int. J. Comput. Vision 89* (September 2010), 266–286. 3

[BCG08] BEN-CHEN M., GOTSMAN C.: Characterizing shape using conformal factors. In *3DOR* (2008), pp. 1–8. 1, 2, 3, 4, 6

[BGSF08] BIASOTTI S., GIORGI D., SPAGNUOLO M., FALCIDIENO B.: Reeb graphs for shape analysis and applications. *Theoretical Computer Science 392*, 1-3 (2008), 5 – 22. 1, 4

[BP06] BIMBO A. D., PALA P.: Content-based retrieval of 3d models. *ACM Trans. Multimedia Comput. Commun. Appl. 2* (February 2006), 20–43. 1

[BPS*10] BIASOTTI S., PATANE' G., SPAGNUOLO M., FALCIDIENO B., BAREQUET G.: Shape approximation by differential properties of scalar functions. *Computers & Graphics-Uk 34* (2010), 252 – 262. 3

[CMEH*04] COLE-MCLAUGHLIN K., EDELSBRUNNER H., HARER J., NATARAJAN V., PASCUCCI V.: Loops in reeb graphs of 2-manifolds. *Discrete Comput. Geom. 32* (July 2004), 231–244. 4

[CSTO03] CHEN D.-Y., SHEN Y.-T., TIAN X.-P., OUHYOUNG M.: On visual similarity based 3d model retrieval. In *Eurographics computer graphics forum* (2003), pp. 223–232. 1, 6

[CZCG04] CARLSSON G., ZOMORODIAN A., COLLINS A., GUIBAS L.: Persistence barcodes for shapes. In *Proceedings of the 2004 Eurographics/ACM SIGGRAPH symposium on Geometry processing* (New York, NY, USA, 2004), SGP '04, ACM, pp. 124–135. 2

[dBvK93] DE BERG M., VAN KREVELD M.: Trekking in the alps without freezing or getting tired. In *AlgorithmsÛESA '93*, Lengauer T., (Ed.), vol. 726 of *Lecture Notes in Computer Science*. Springer Berlin / Heidelberg, 1993, pp. 121–132. 4

[DGG03] DEY T., GIESEN J., GOSWAMI S.: Shape segmenta-

tion and matching with flow discretization. In *Algorithms and Data Structures*, vol. 2748 of *Lecture Notes in Computer Science*. Springer Berlin / Heidelberg, 2003, pp. 25–36. 2

[EK03] ELAD A., KIMMEL R.: On bending invariant signatures for surfaces. *Pattern Analysis and Machine Intelligence, IEEE Transactions on 25*, 10 (2003), 1285 – 1295. 2

[GBP07] GIORGI D., BIASOTTI S., PARABOSCHI L.: Shape retrieval contest 2007: Watertight models track, 2007. 6

[GSCO07] GAL R., SHAMIR A., COHEN-OR D.: Pose-oblivious shape signature. *IEEE Transactions on Visualization and Computer Graphics 13*, 2 (2007), 261–271. 2

[HK03] HAMZA A. B., KRIM H.: Geodesic object representation and recognition. In *Discrete Geometry for Computer Imagery*, Nyström I., Sanniti di Baja G., Svensson S., (Eds.), vol. 2886 of *Lecture Notes in Computer Science*. Springer Berlin / Heidelberg, 2003, pp. 378–387. 3

[HSKK01] HILAGA M., SHINAGAWA Y., KOHMURA T., KUNII T. L.: Topology matching for fully automatic similarity estimation of 3d shapes. In *Proceedings of the 28th annual conference on Computer graphics and interactive techniques* (New York, NY, USA, 2001), SIGGRAPH '01, ACM, pp. 203–212. 1, 3, 4

[JZ07] JAIN V., ZHANG H.: A spectral approach to shape-based retrieval of articulated 3d models. *Comput. Aided Des. 39* (May 2007), 398–407. 2

[KFR03] KAZHDAN M., FUNKHOUSER T., RUSINKIEWICZ S.: Rotation invariant spherical harmonic representation of 3d shape descriptors. In *SGP '03: Proceedings of the 2003 Eurographics/ACM SIGGRAPH symposium on Geometry processing* (Aire-la-Ville, Switzerland, Switzerland, 2003), Eurographics Association, pp. 156–164. 2, 6

[KPYL05] KIM D., PARK I., YUN I., LEE S.: A new mpeg-7 standard: Perceptual 3-d shape descriptor. In *Advances in Multimedia Information Processing - PCM 2004*, Aizawa K., Nakamura Y., Satoh S., (Eds.), vol. 3332 of *Lecture Notes in Computer Science*. Springer Berlin / Heidelberg, 2005, pp. 238–245. 3

[MDSB02] MEYER M., DESBRUN M., SCHRODER P., BARR A. H.: Discrete differential-geometry operators for triangulated 2-manifolds. *Visualization and mathematics 3* (2002), 1–26. 3

[MDTS09] MADEMLIS A., DARAS P., TZOVARAS D., STRINTZIS M. G.: 3d object retrieval using the 3d shape impact descriptor. *Pattern Recogn. 42* (November 2009), 2447–2459. 2

[PPPT08] PAPADAKIS P., PRATIKAKIS I., PERANTONIS S., THEOHARIS T.: 3d object retrieval using an efficient and compact hybrid shape descriptor. In *Eurographics Workshop on 3D object retrieval* (2008), pp. 9–16. 2

[PPTP09] PAPADAKIS P., PRATIKAKIS I., THEOHARIS T., PERANTONIS S.: Panorama: A 3d shape descriptor based on panoramic views for unsupervised 3d object retrieval. *International Journal of Computer Vision* (2009). 2

[Rus07] RUSTAMOV R. M.: Laplace-beltrami eigenfunctions for deformation invariant shape representation. In *Proceedings of the fifth Eurographics symposium on Geometry processing* (Aire-la-Ville, Switzerland, Switzerland, 2007), Eurographics Association, pp. 225–233. 2

[RWP06] REUTER M., WOLTER F.-E., PEINECKE N.: Laplace-beltrami spectra as [‘]shape-dna' of surfaces and solids. *Computer-Aided Design 38*, 4 (2006), 342 – 366. Symposium on Solid and Physical Modeling 2005. 2

[SKK91] SHINAGAWA Y., KUNII T. L., KERGOSIEN Y. L.: Surface coding based on morse theory. *IEEE Comput. Graph. Appl. 11* (September 1991), 66–78. 4

[SMKF04] SHILANE P., MIN P., KAZHDAN M., FUNKHOUSER T.: The Princeton Shape Benchmark. In *Shape Modeling and Applications* (2004), pp. 167–178. 1

[SSA08] SANROMÀ G., SERRATOSA F., ALQUÉZAR R.: Hybrid genetic algorithm and procrustes analysis for enhancing the matching of graphs generated from shapes. In *Structural, Syntactic, and Statistical Pattern Recognition*, da Vitoria Lobo N., Kasparis T., Roli F., Kwok J., Georgiopoulos M., Anagnostopoulos G., Loog M., (Eds.), vol. 5342 of *Lecture Notes in Computer Science*. Springer Berlin / Heidelberg, 2008, pp. 298–307. 5

[SSGD03] SUNDAR H., SILVER D., GAGVANI N., DICKINSON S.: Skeleton based shape matching and retrieval. In *Shape Modeling International, 2003* (May 2003), pp. 130 – 139. 2

[STP10] SFIKAS K., THEOHARIS T., PRATIKAKIS I.: Rosy+: 3d object pose normalization based on pca andăreflective object symmetry with application in 3d object retrieval. *International Journal of Computer Vision* (2010), 1–18. 10.1007/s11263-010-0395-x. 2

[TS05] TUNG T., SCHMITT F.: The augmented multiresolution reeb graph approach for content-based retrieval of 3d shapes. *International Journal of Shape Modeling 11*, 1 (2005), 91–120. 3, 6

[TSK97] TAKAHASHI S., SHINAGAWA Y., KUNII T. L.: A feature-based approach for smooth surfaces. In *Proceedings of the fourth ACM symposium on Solid modeling and applications* (New York, NY, USA, 1997), SMA '97, ACM, pp. 97–110. 4

[TV98] TARASOV S. P., VYALYI M. N.: Construction of contour trees in 3d in o(n log n) steps. In *Proceedings of the fourteenth annual symposium on Computational geometry* (New York, NY, USA, 1998), SCG '98, ACM, pp. 68–75. 4

[TV08] TANGELDER J., VELTKAMP R.: A survey of content based 3d shape retrieval methods. *Multimedia Tools and Applications 39* (2008), 441–471. 1

[TVD09] TIERNY J., VANDEBORRE J.-P., DAOUDI M.: Partial 3d shape retrieval by reeb pattern unfolding. *Computer Graphics Forum 28*, 1 (2009), 41–55. 3

[WWJ*06] WANG S., WANG Y., JIN M., GU X., SAMARAS D.: 3d surface matching and recognition using conformal geometry. In *Computer Vision and Pattern Recognition, 2006 IEEE Computer Society Conference on* (2006). 2

[XHGC07] XIANG P., HUA C., GANG F., CHUAN Z.: Pose insensitive 3d retrieval by poisson shape histogram. In *Computational Science Ű ICCS 2007*, Shi Y., van Albada G., Dongarra J., Sloot P., (Eds.), vol. 4488 of *Lecture Notes in Computer Science*. Springer Berlin / Heidelberg, 2007, pp. 25–32. 2

[ZP02] ZAHARIA T., PRETEUX F.: Shape-based retrieval of 3d mesh models. In *Multimedia and Expo, 2002. ICME '02. Proceedings. 2002 IEEE International Conference on* (2002). 2

[ZSM*05] ZHANG J., SIDDIQI K., MACRINI D., SHOKOUFANDEH A., DICKINSON S.: Retrieving articulated 3-d models using medial surfaces and their graph spectra. In *Energy Minimization Methods in Computer Vision and Pattern Recognition*, Rangarajan A., Vemuri B., Yuille A., (Eds.), vol. 3757 of *Lecture Notes in Computer Science*. Springer Berlin / Heidelberg, 2005, pp. 285–300. 2